SUPPORTING INFORMATION

The Electrochemical Approach to Concerted Proton-Electron Transfers in the Oxidation of Phenols in Water

Cyrille Costentin, Cyril Louault, Marc Robert and Jean-Michel Savéant
Contribution from the Laboratoire d'Electrochimie Moléculaire, Unité Mixte de Recherche Université - CNRS No 7591, Université Paris - Diderot, Bâtiment Lavoisier, 15 rue Jean de Baïf, 75205 Paris Cedex 13, France.

Table of Contents

1. Experimental Section

1.1. Chemicals

Phenol (Merck, > 99,5 %) was used as received. Sodium dihydrogen phosphate dihydrate (Fluka, > 99%), boric acid (Aldrich) and citric acid (Aldrich, 99%) were used to prepare buffers. Solutions were prepared with either deionized water or deuterium oxide (Euriso-top, 99,90%). KNO_3 (Aldrich, > 99 %) was used as supporting electrolyte.

1.2. Instrumentation

The working electrode was a 3-mm diameter glassy carbon electrode disk (Tokai) carefully polished with 3 µm and 1 µm DP-Paste, M (Struers) for 2 min and ultrasonically rinsed in ethanol 96% vol. for 1 min before each run. The counter-electrode was a platinum wire and the reference electrode an aqueous saturated calomel electrode (SCE). The potentiostat was an Autolab PGSTAT 12. The solution was deoxygenated by bubbling argon prior to each experiment and an argon flow was kept over the solution during the whole experiment. All solutions contained 0.5 M of the supporting electrolyte (KNO_3).

The *pH* measurements in H_2O and D_2O were done using a Hanna HI 221 pH-meter and a Bioblock combined glass/AgCl electrode (ø = 6 mm). *pD* is obtained by adding 0.4 to the value given by the glass electrode (1S).

2. Self Inhibition

Self-inhibition (2S) produces dramatic effects on the cyclic voltammetric responses as can be seen in figure 1S, which shows a rapid decrease of the current upon repetitive cycling.

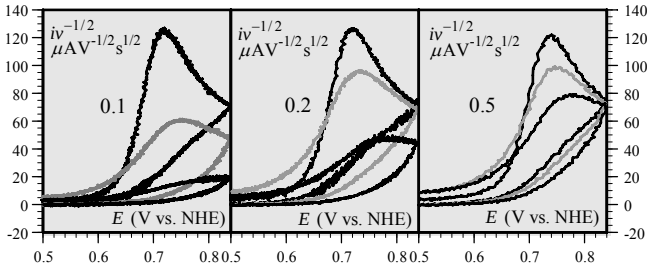

Fig. 1S. Cyclic voltammetry of 1 mM PhOH in a 0.05 M Britton Robinson buffer at *pH* = 10.7. Self-inhibition produced by successive potential scans: from top to bottom: 1st, 2nd and 3rd scan respectively. The number on each diagram is the scan rate in V/s.

The rate of self-inhibition decreases upon raising the scan rate, in line with the charge passed during the voltammogram, and hence the production of the inhibiting film, decreasing as $1/\sqrt{\text{scan rate}}$ (3S). Self-inhibition during the first scan (figure 2S) is a decreasing function of the scan rate, *v*, and an increasing function of phenol concentration, C^0.

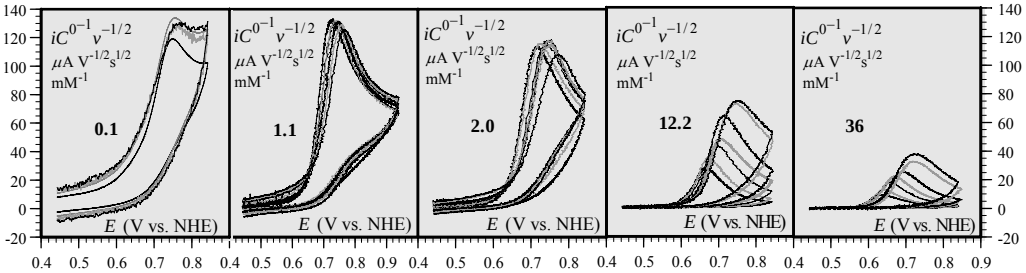

Fig. 2S. Cyclic voltammetry of PhOH in a 0.05 M Britton Robinson buffer at *pH* = 10.7. Self-inhibition in the first potential scan as a function of phenol concentration (number in each diagram in mM) and scan rates: from left to right: 0.1, 0.2, 0.5, 1, 2, 5, 10 (V/s) with the exception of the first diagram where the scan rates are 1, 2, 5, 10 V/s.

We see that the effects of inhibition can be neglected at concentrations below 1 mM and scan rates above 0.1 V/s. The validity of this estimation appears more precisely on the diagrams in figure 3S, which show the variation of the peak potential with scan rate and phenol concentration, taking into account that the peak potential is expected to obey equation (1), in the text, for a reaction in which fast and reversible electron and proton transfers precede a rate-determining dimerization.

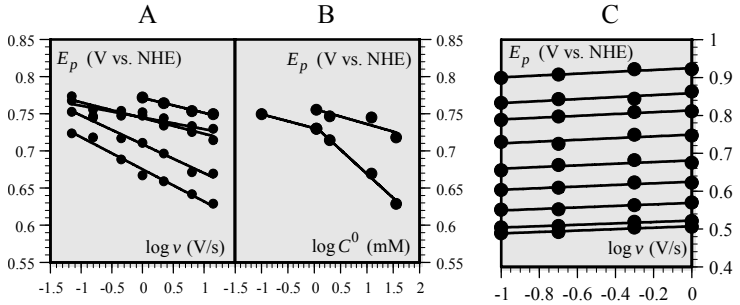

Fig. 3S. Cyclic voltammetry of PhOH in a 0.05 M Britton Robinson buffer at *pH* = 10.7. A: variation of the peak potential with scan rate at various concentrations (mM); from bottom to top: 0.1, 1.1, 2.0, 12.2, 36. B: variation of the peak potential concentration at two scan rates (V/s): 0.2 (bottom), 10 (top). C: verification the absence of self-inhibition at 0.2 mM and 0.2 V/s by checking equation (1) by means of the variation of the peak potential with scan over the *pH* range: from top to bottom: 3, 4, 5, 6, 7, 8, 9, 10, and 11 ($\partial E_p / \partial(\log v) = 22.0 \pm 2.5$ mV)

The slopes in the figure 3SA diagram are close to the theoretical value of 19.7 mV per decade of scan rate up to 2 mM phenol concentration. Figure 3SB shows that the theoretical slope of 19.7 mV per decade of concentration is observed over the whole concentration range at a scan rate of 10 V/s whereas this is only the case below 1 mM at a scan rate of 0.2 V/s. Figure 3SC shows the verification that self-inhibition is indeed negligible at 0.2 mM and 0.2 V/s by checking equation (1) by means of the variation of the peak potential with scan over the *pH* range. The slope of the linear variation of the peak potential with the log of scan rate, 22.0 ± 2.5 mV is indeed close to the theoretical value of 20 mV characterizing a rate-determining dimerization step following a Nernstian electron transfer step (4S).

3. Theoretical Predictions for the Various Mechanisms

3.1 General

We examine in the next sections the main kinetic characteristics of each of the possible reaction pathways. Each section is organized so as to first state the main characteristics, followed by the demonstration of their validity. The present section is devoted to the principles, equations, definitions of variables and parameters common to all pathways.

The concentrations of the various reacting species are time (t) and space functions that are assume to obey the Fick's second law of linear diffusion (planar electrode; *x*: distance to the electrode surface) with or without a kinetic term representing the coupling of diffusion with homogeneous reactions:

$$\frac{\partial[\text{reactant}]}{\partial t} = D_{\text{reactant}} \frac{\partial^2[\text{reactant}]}{\partial x^2} + \textit{kinetic term}$$ (D_{reactant} : diffusion coefficient of the subscript species)

Dealing with cyclic voltammetry, one of the boundary conditions at the electrode solution-interface is, in all following cases, the expression of the linear scanning of the electrode-solution interface ($x = 0$):

$E = E_i + vt$ during the forward scan (v: scan rate, E_i: starting potential) and $E = E_f + v(t - t_R)$ during the reverse scan (E_f: reversing potential, $t_R = (E_f - E_i)/v$: reversing time).

In order to make the competition key-parameters emerge, it is useful to formulate the variables, parameters and equations in a dimensionless manner, starting with time and space:

$$\tau = \frac{Fv}{RT} t \ , \ y = x\sqrt{\frac{Fv}{RTD}}$$

D is the diffusion coefficient of phenol, which we assume to be practically equal to that of the phenoxyl radical and the phenoxide ion. When another reactant has an obviously different diffusion coefficient, as in the case of proton or OH^- ion, its ratio with *D* is an additional dimensionless parameter to be taken into account: $\delta_H = D_{H^+}/D$, $\delta_{OH} = D_{OH^-}/D$, $\delta_Z = D_Z/D$.

The dimensionless electrode potential is defined as:

$\xi = \frac{F}{RT}(E - E^0)$ by reference to the standard potential, E^0, of the pathway under examination.

Having defined:

$$\tau_R = \frac{Fv}{RT} t_R \ , \ u_i = \frac{F}{RT}(E_i - E^0) \ , \ u_f = \frac{F}{RT}(E_f - E^0)$$

The linear potential scanning conditions become:

$0 < \tau < \tau_R$: $\xi = u_i + \tau$

$\tau_R < \tau < 2\tau_R$: $\xi = u_f - (\tau - \tau_R)$

The concentrations of reactants are normalized toward the bulk concentration of phenol, C^0:

$$a = \frac{[\text{ArOH}]}{C^0} \ , \ b = \frac{[\text{ArO}^-]}{C^0} \ , \ c = \frac{[\text{ArO}^\bullet]}{C^0} \ , h = \frac{[\text{H}^+]}{C^0} \ , \ oh = \frac{[\text{OH}^-]}{C^0} \ , \ z = \frac{[\text{Z}]}{C^0} \ , \ zh = \frac{[\text{ZH}]}{C^0}$$

The bulk concentrations of other reactants are also normalized toward the bulk concentration of phenol:

$b^0 = \frac{[\text{ArO}^-]^0}{C^0}$, $h^0 = \frac{[\text{H}^+]^0}{C^0}$, $oh^0 = \frac{[\text{OH}^-]^0}{C^0}$, whereas the bulk concentration of $\text{ArO}^\bullet$ is always equal to zero.

The current flowing through the electrode, *i*, is in general the sum of two contribution representing the oxidation of phenol and phenoxide ion, respectively, which both produce the phenoxyl radical. Thus:

$$\frac{i}{FS} = D\left\{\left(\frac{\partial[\text{ArOH}]}{\partial x}\right)_{x=0} + \left(\frac{\partial[\text{ArO}^-]}{\partial x}\right)_{x=0}\right\} = -D\left(\frac{\partial[\text{ArO}^\bullet]}{\partial x}\right)_{x=0}$$ (*S* is the electrode surface area)

The dimensionless current is defined as:

$$\psi = \frac{i}{FSC^0\sqrt{D}\sqrt{\frac{Fv}{RT}}} = \left(\frac{\partial a}{\partial y}\right)_{y=0} + \left(\frac{\partial b}{\partial y}\right)_{y=0} = -\left(\frac{\partial c}{\partial y}\right)_{y=0}$$

In the following, it will be useful to express the relationship between certain concentrations in the bulk and their counterpart in the solution, to introduce the convoluted dimensionless current with the function $1/\sqrt{\pi\tau}$, characteristic of linear diffusion:

$$\mathcal{I}\psi = \frac{1}{\sqrt{\pi}} \int_0^\tau \frac{\psi}{\sqrt{\tau - \eta}} d\eta$$

The above linear potential scanning conditions have to be taken into account in the calculation of the convolution integral. The procedures we used for numerical calculation of the integral equations expressing the cyclic voltammetric waves in dimensionless terms are described in section 3.6. In several cases, the dimensionless cyclic voltammograms may be alternatively simulated using commercial packages like DigiElch (5S) (the response of the EPT pathway in section 2.2 was simulated according to this procedure). This is not the case with concerted pathways, which involve a termolecular (electrode + two molecules, actually) step at least in one direction, which are not implemented in these type of packages.

The above partial derivative equation may thus be writen:

$$\frac{\partial[\text{dimensionless conc.}]}{\partial t} = \frac{\partial^2[\text{dimensionless conc.}]}{\partial x^2} + \textit{dimensionless kinetic term}$$

The rate constants in the dimensionless kinetic term are normalized as

$\lambda = \frac{RT}{F}\frac{k_{1st}}{v}$, for a first-order reaction and $\lambda = \frac{RT}{F}\frac{k_{2nd}C^0}{v}$ for a 2nd order-reaction. In the case of the dimerization reaction, which is involved in all mechanisms that we consider: $\lambda_{dim} = \frac{RT}{F}\frac{2k_{dim}C^0}{v}$.

Integration of these partial derivative equations, leading to the expression of the various time- and space-dependent reactant concentrations and hence to the sough expression of the current, requires taking into account the following set of initial and boundary conditions:

$\tau = 0,\ y \geq 0$ and : $y = \infty, \tau \geq 0 : a = 1, b = b^0, c = 0, h = h^0, oh = oh^0$

$y = 0, \tau \geq 0 : \left(\frac{\partial a}{\partial y}\right)_0 + \left(\frac{\partial b}{\partial y}\right)_0 = -\left(\frac{\partial c}{\partial y}\right)_0 (= \psi), \left(\frac{\partial oh}{\partial y}\right)_0 = 0$ (the subscript 0 stands for $y = 0$),

and, in the case where the corresponding species are not involved directly in the electron transfer step, i.e. in the PET pathways:

$$\left(\frac{\partial h}{\partial y}\right)_0 = 0,\ \left(\frac{\partial zh}{\partial y}\right)_0 = 0,\ \left(\frac{\partial z}{\partial y}\right)_0 = 0$$

Otherwise:

$$\delta_H\left(\frac{\partial h}{\partial y}\right)_0 = -\psi,\ \delta_Z\left(\frac{\partial z}{\partial y}\right)_0 = \psi = -\delta_Z\left(\frac{\partial zh}{\partial y}\right)$$

Still for $y = 0, \tau \geq 0$: another boundary condition is a relationship describing either the thermodynamics of the electron transfer step (Nernst law) if this is fast or its kinetics if not.

As indicated in the manuscript, the electron transfer rate law has been approximated by a Butler-Volmer expression with a transfer coefficient equal to 0.5.

In the case of the PET pathways:

$$\frac{i}{FS} = k_S \exp\left[\frac{F}{2RT}\left(E - E^0\right)\right]\left\{\left[\text{ArO}^-\right]_{x=0} - \left[\text{ArO}^\bullet\right]_{x=0} \exp\left[-\frac{F}{RT}\left(E - E^0\right)\right]\right\},$$

corresponding to a "bimolecular" (electrode+ 1 molecule) step in both directions.
and in the case of the CPET pathways:

$$\frac{i}{FS} = k_S \exp\left[\frac{F}{2RT}\left(E - E^0\right)\right]\left\{[\text{ArO}]_{x=0}\frac{[\text{Z}]_{x=0}}{C_S} - \left[\text{ArO}^\bullet\right]_{x=0}\frac{[\text{ZH}]_{x=0}}{C_S}\exp\left[-\frac{F}{RT}\left(E - E^0\right)\right]\right\},$$

corresponding to a "termolecular" (electrode+ 2 molecules) in both directions. In the case where Z is water, its concentration is replaced by its activity, equal to unity, by conventional definition of k_S, the standard rate constant. The forward step is then "bimolecular" and the reverse step, "termolecular" (for a discussion of termolecular kinetics in electron transfer reactions concerted with the breaking of a bond see references 6S and 7S). Then:

$$\frac{i}{FS} = k_S \exp\left[\frac{F}{2RT}\left(E - E^0\right)\right]\left\{[\text{ArO}]_{x=0} - \left[\text{ArO}^\bullet\right]_{x=0}\frac{\left[\text{H}^+\right]_{x=0}}{C_S}\exp\left[-\frac{F}{RT}\left(E - E^0\right)\right]\right\}$$

The introduction of the standard concentration, C_S (that we take equal to 1 mol/L.), in the above equations allows one to keep the same definition, throughout the various cases, of the standard rate constant, k_S, with the same units (usually cm/s).

The exact meaning of the standard rate constant, k_S, and of the standard potential E^0 depends on the particular pathway under examination as made clear in the following sections.

In the first case, the dimensionless expression of the rate law is the following.

$$\psi = \Lambda \exp\left[\frac{F}{2RT}\left(E - E^0\right)\right]\left\{b_0 - c_0 \exp\left[-\frac{F}{RT}\left(E - E^0\right)\right]\right\}$$

and in the second:

$$\psi = \Lambda \exp\left[\frac{F}{2RT}\left(E - E^0\right)\right]\left\{a_0 z_0 \frac{C^0}{C_S} - c_0 z h_0 \frac{C^0}{C_S}\exp\left[-\frac{F}{RT}\left(E - E^0\right)\right]\right\}$$

or, for water:

$$\psi = \Lambda \exp\left[\frac{F}{2RT}\left(E - E^0\right)\right]\left\{a_0 - c_0 h_0 \frac{C^0}{C_S}\exp\left[-\frac{F}{RT}\left(E - E^0\right)\right]\right\}$$

introducing a new dimensionless parameter that measures the competition between electron transfer and diffusion:

$$\Lambda = \frac{k_S}{\sqrt{D}\sqrt{\frac{Fv}{RT}}}$$

the definition of which remains the same whatever the case.

3.2. The OH⁻-PET pathway in unbuffered water

The dimensionless expression of the cyclic voltammetric responses expected for this mechanism is given by the following integral equation.

$$\frac{\psi^{2/3}\exp\left(-\xi_{dim}\right)}{1-\mathcal{I}\psi-\psi^{2/3}\exp\left(-\xi_{dim}\right)} = \left(\kappa/\delta_{OH}\right)\left[\kappa oh^0/\left(1+\kappa oh^0\right)-\mathcal{I}\psi-\psi^{2/3}\exp\left(-\xi_{dim}\right)\right]+\kappa oh^0 \qquad (1S)$$

$\xi_{dim} = \left(F/RT\right)\left(E-E_{PET}^{dim}\right)$ is a dimensionless expression of the driving force of the reaction as measured by the difference between the electrode potential, E, and a characteristic potential, $E_{PET}^{dim} = E_{PET}^0 - \left(RT/3F\right)\ln\left[\left(2RT/3F\right)\left(2k_{dim}C^0/v\right)\right]$, which derives from the standard potential E_{PET}^0 by correcting for the follow-up dimerization, introducing its rate constant, $2k_{dim}$ and the scan rate, v. E_{PET}^{dim} is immediately derived from the horizontal part of the plot in figure 1b by: $E_{PET}^{dim} = E_{p,PET}^{at\ v} - 0.903RT/F$.

The other parameters are dimensionless measures of the initial *pH* and of the ratio of the diffusion coefficients $\kappa oh^0 = K_{\mathrm{ArOH}}/\left[\mathrm{H^+}\right]^0$ and $\kappa/\delta_{OH} = K_{\mathrm{ArOH}}C^0D/\left(K_W D_{\mathrm{OH^-}}\right)$ (K_W : water autoprotolysis constant)

How can one gets to this expression of the cyclic voltammetric response?

The partial derivatives equations (Fick's second law) relative to the various reactants may be expressed in dimensionless form as:

$$\frac{\partial a}{\partial \tau} = \frac{\partial^2 a}{\partial y^2} - \lambda_{-p} oh \times a + \lambda_p b\ ,\ \frac{\partial b}{\partial \tau} = \frac{\partial^2 b}{\partial y^2} + \lambda_{-p} oh \times a - \lambda_p b\ ,\ \frac{\partial oh}{\partial \tau} = \delta_{OH}\frac{\partial^2 oh}{\partial y^2} - \lambda_{-p} oh \times a + \lambda_p b\ ,\ \frac{\partial c}{\partial \tau} = \frac{\partial^2 c}{\partial y^2} - \lambda_{dim} c^2\ ,$$

In the latter equation, dimerization is so fast, and therefore λ_{dim} is so large in the range of scan rate considered here, that a steady-state is achieved in which diffusion and dimerization compensate each other leading to the so-called "pure kinetic" conditions (4). Then:

$$\frac{\partial^2 c}{\partial y^2} = \lambda_{dim} c^2 \text{ and thus } \frac{\partial c}{\partial y}\frac{\partial^2 c}{\partial y^2} = \lambda_{dim}\frac{\partial c}{\partial y}c^2$$

Integration leads to:

$$\left(\frac{\partial c}{\partial y}\right)^2 = \frac{2\lambda_{dim}}{3}c^3\ ,\ \text{i.e. } \psi^2 = \frac{2\lambda_{dim}}{3}c_0^3 \text{ or } c_0 = \left(\frac{3}{2\lambda_{dim}}\right)^{1/3}\psi^{2/3}$$

Since the protonation/ deprotonation reactions are fast:

$$\frac{\partial oh}{\partial \tau} \simeq 0 \simeq \delta\frac{\partial oh}{\partial \tau} \text{ and thus: } \frac{\partial \delta oh}{\partial \tau} \simeq \frac{\partial^2 \delta oh}{\partial y^2} - \lambda_{-p} oh \times a + \lambda_p b$$

It follows that:

$$\frac{\partial\left(a+b\right)}{\partial \tau} = \frac{\partial^2\left(a+b\right)}{\partial y^2}\ ,\ \frac{\partial\left(b+\delta oh\right)}{\partial \tau} = \frac{\partial^2\left(b+\delta oh\right)}{\partial y^2}$$

Integration of these two equations leads to:

$a_0 + b_0 = 1 - \mathcal{I}\psi$ and $b_0 + \delta_{OH} oh_0 = b^0 + \delta_{OH} oh^0 - \mathcal{I}\psi$.

The coupled proton transfer reaction is assumed to be at equilibrium at all times and distances from the electrode:

$$\frac{b}{a \times oh} = \kappa\ ,\ \kappa = \frac{K_{\mathrm{ArOH}}C^0}{K_W} \text{ since: } \frac{\left[\mathrm{ArO^-}\right]\left[\mathrm{H^+}\right]}{\left[\mathrm{ArOH}\right]} = K_{\mathrm{ArOH}}, \frac{\left[\mathrm{ArO^-}\right]}{\left[\mathrm{ArOH}\right]} = \frac{K_{\mathrm{ArOH}}}{K_W}\left[\mathrm{OH^-}\right] = \frac{K_{\mathrm{ArOH}}C^0}{K_W}\frac{\left[\mathrm{OH^-}\right]}{C^0}$$

($K_{\mathrm{ArOH}} = 10^{-pK_{\mathrm{ArOH}}}$),

$$oh^0 = \frac{\left[\mathrm{OH^-}\right]^0}{C^0} = \frac{K_W}{C^0\left[\mathrm{H^+}\right]^0}\ ,\ \kappa oh^0 = \frac{K_{\mathrm{ArOH}}}{\left[\mathrm{H^+}\right]^0}$$

Therefore:

$$a_0 + b_0 = b_0\frac{1+\kappa oh_0}{\kappa oh_0}$$

It follows that:

$$b_0\frac{1+\kappa oh_0}{\kappa oh_0} = 1 - \mathcal{I}\psi \text{ , with } b^0 = \frac{\kappa oh^0}{1+\kappa oh^0}$$

The oxidation of phenol goes entirely through the phenoxide ion in the framework of the PET mechanism and we assume that the electron transfer is fast thus obeying the Nernst law, which reads in dimensionless terms

$$b_0 = c_0\exp\left(-\xi\right)$$

and therefore, on the one hand:

$$b_0 = \left(\frac{3}{2\lambda_{dim}}\right)^{1/3} \psi^{2/3} \exp(-\xi) = \psi^{2/3} \exp(-\xi_{dim}) \text{ with: } \xi_{dim} = \xi + \frac{1}{3}\ln\left(\frac{2\lambda_{dim}}{3}\right)$$

while, on the other: $b_0 + \delta_{OH} o h_0 = b^0 + \delta_{OH} o h^0 - \mathcal{I}\psi$,

i.e.:

$$b_0 = (1 - \mathcal{I}\psi) \frac{\frac{\kappa}{\delta_{OH}}\left(\frac{\kappa o h^0}{1+\kappa u^0} - b_0 - \mathcal{I}\psi\right) + \kappa o h^0}{1 + \frac{\kappa}{\delta_{OH}}\left(\frac{\kappa o h^0}{1+ohu^0} - b_0 - \mathcal{I}\psi\right) + \kappa o h^0}$$

Combination of these two expressions of b_0 finally leads to equation (1S), which can be solved numerically according to the procedure described in section 3.6.

3.3. The H_2O-CPET pathway in unbuffered water

The main purpose here is to established equation 2S below

$$\psi = p \exp\left(\frac{\xi^*_{dim}}{2}\right)\left[1 - \mathcal{I}\psi - \psi^{2/3}\mathcal{I}\psi \exp\left(-\xi^*_{dim}\right)\right] \qquad (2S)$$

$$\text{with : } \xi^*_{dim} = \xi + \ln\left\{\frac{\left(\frac{4k_{dim}C^0}{3}\frac{RT}{Fv}\right)^{1/3}}{\frac{C^0}{C_S}\sqrt{\frac{D}{D_{H^+}}}}\right\} \text{ and } p = \Lambda\sqrt{\frac{\frac{C^0}{C_S}\sqrt{\frac{D}{D_{H^+}}}}{\left(\frac{2\lambda_{dim}}{3}\right)^{1/3}}} = \frac{k_S^{CPET}\left(\frac{C^0}{C_S}\right)^{1/2}}{D^{1/4}D_{H^+}{}^{1/4}\left(\frac{Fv}{RT}\right)^{1/3}\left(\frac{4k_{dim}C^0}{3}\right)^{1/6}}$$

which corresponds to the horizontal set of data points in figure 3a. It is also the equation we used to make the successful simulation of the voltammetric responses in figure 4, leading to the determination of k^{CPET}_{S,H_2O}, which was made possible because p has an intermediate value (0.5 at 0.2 V/s) that reflects a mixed kinetic control by electron transfer and dimerization.

With the same initial and boundary conditions as earlier and, noting that in the considered pH range ($pH << pK_{ArOH}$), the dimensionless partial derivatives equations of interest are now:

$$\frac{\partial a}{\partial \tau} = \frac{\partial^2 a}{\partial y^2} \text{ and } \frac{\partial h}{\partial \tau} = \delta_H \frac{\partial^2 h}{\partial y^2}$$

leading, after integration to: $a_0 = 1 - \mathcal{I}\psi$ and $h_0 = h^0 + \frac{\mathcal{I}\psi}{\sqrt{\delta_H}}$. Dimerization of the phenoxyl radicals is involved in the same way as in the preceding section, leading similarly to $c_0 = (3/2\lambda_{dim})^{1/3}\psi^{2/3}$

Applying now the Butler-Volmer law,

$$\psi = \Lambda \exp\left[\frac{F}{2RT}\left(E - E^{0,H_2O}_{CPET}\right)\right]\left\{a_0 - c_0 h_0 \frac{C^0}{C_S}\exp\left[-\frac{F}{RT}\left(E - E^{0,H_2O}_{CPET}\right)\right]\right\} \quad \text{with: } \Lambda = \frac{k^{CPET}_{S,H_2O}}{\sqrt{D}\sqrt{\frac{Fv}{RT}}}$$

One obtain the following dimensionless expression of the voltammetric responses for the H_2O-CPET pathway

$$\psi = \Lambda \exp\left[\frac{F}{2RT}\left(E - E^{0,H_2O}_{CPET}\right)\right]\left[1 - \mathcal{I}\psi - \psi^{2/3}\left(h^0 + \frac{\mathcal{I}\psi}{\sqrt{\delta}}\right)\exp\left\{-\frac{F}{RT}\left[E - \left(E^{0,H_2O}_{CPET} + \frac{RT}{F}\ln\frac{C^0}{C_S} - \frac{RT}{3F}\ln\frac{2\lambda_{dim}}{3}\right)\right]\right\}\right]$$

This is a general equation applicable over the whole pH domain ranging from 2 to 10 (see figure 3 in the main text)

There are two limiting situations according to the magnitude of h^0 :

If $h^0 >> \frac{\mathcal{I}\psi}{\sqrt{\delta_H}}$, i.e.: $\left[H^+\right]^0 >> \mathcal{I}\psi C^0\sqrt{D/D_H}$:

the initial concentration of protons is large enough for not being perturbed by their production from phenol oxidation, as it is the case below pH 3. Then, dimensionless expression of the voltammetric response is:

$$\psi = p' \exp\left(\frac{\xi'_{dim}}{2}\right)\left[1 - \mathcal{I}\psi - \psi^{2/3}\exp\left(-\xi'_{dim}\right)\right]$$

$$\text{with } \xi'_{dim} = \xi + \ln\left\{\frac{\left(\frac{4k_{dim}C^0}{3}\frac{RT}{Fv}\right)^{1/3}}{\left[H^+\right]^0/C_S}\right\} \text{ and } p' = \Lambda\left\{\frac{\left[H^+\right]^0/C_S}{\left(\frac{2\lambda_{dim}}{3}\right)^{1/3}}\right\}^{1/2} = \frac{k^{CPET}_{S,H_2O}\left(\left[H^+\right]^0/C_S\right)^{1/2}}{D^{1/2}(Fv/RT)^{1/3}\left(4k_{dim}C^0/3\right)^{1/6}}$$

The parameter p' is a measure of the competition between dimerization ($p' \to \infty$) and electron transfer ($p' \to 0$) for the kinetic control of the whole process. The peak potential dimerization-controlled wave obtained in the first case follows the dimerization-modified Pourbaix variation with pH that was indeed observed over the whole pH range in buffered medium and below pH 3 in

unbuffered water. That dimerization controls the overall kinetics in these circumstances is essentially the result of the large value of k_{S,H_2O}^{CPET}, 25 cm/s as will be established further on. The value of the parameter *p'* in unbuffered water at *pH* 3 is indeed 7 (using the parameter values in Table 1 of the main text) leaving no chance to electron transfer to participate in the kinetic control.

A more interesting situation for our purpose of characterizing the kinetics of the H_2O-CPET pathway is when, conversely, $h^0 << \frac{\mathcal{I}\psi}{\sqrt{\delta_H}}$, i.e.: $\left[H^+\right]^0 << \mathcal{I}\psi C^0\sqrt{\frac{D}{D_{H^+}}}$, leading to equation (2S).

3.4. The PO_4H^{2-}-PET pathway

Derivation of the dimensionless expression of the voltammetric responses under the assumption that electron transfer is so fast that it remains at equilibrium, obeying the Nernst law, is similar to the derivation in section 3.2. The rate-limiting factors are then phenoxyl dimerization and diffusion of the buffer components when these are in low concentration. The pertinent partial derivative equations are, in dimensionless form:

$$\frac{\partial(a+b)}{\partial\tau}=\frac{\partial^2(a+b)}{\partial y^2},\ \frac{\partial(b+\delta_Z z)}{\partial\tau}=\frac{\partial^2(b+\delta_Z z)}{\partial y^2},\ \frac{\partial(z-zh)}{\partial\tau}=\frac{\partial^2(z-zh)}{\partial y^2}$$

leading after integration to:

$a_0+b_0=1-\mathcal{I}\psi$, $b_0+\delta z_0=b^0+\delta_Z z^0-\mathcal{I}\psi$

and, considering for simplicity that the *pH* is set at the *pK* of the buffer, i.e. $[Z]^0=[ZH]^0$,to:

$z_0+zh_0=z^0+zh^0=2z^0=2zh^0$

The fate of the phenoxyl radical is the same as in section 3.2 leading to:

$$c_0=\left(\frac{3}{2\lambda_{dim}}\right)^{1/3}\psi^{2/3}$$

Application of the dimensionless Nernst law leads to a first equation relating b_0 to ψ:

$$b_0=\psi^{2/3}\exp\left(-\xi_{dim}\right)$$

where $\xi_{dim}=\xi+\frac{1}{3}\ln\left(\frac{2\lambda_{dim}}{3}\right)=\xi+\frac{1}{3}\ln\left(\frac{4k_{dim}C^0}{3}\frac{RT}{Fv}\right)$ is the same dimerization-corrected dimensionless potential scale as introduced earlier.

A second important, already mentioned, equation relates b_0, z_0 and ψ

$b_0+\delta z_0=b^0+\delta_Z z^0-\mathcal{I}\psi$

A third equation, relating b_0, z_0 and ψ is obtained from the assumption that coupled protonation/ deprotonation reaction is at equilibrium at all times and distances from the electrode, and particularly at the electrode surface:

$\frac{b_0\times zh_0}{a_0\times z_0}=\kappa$, with $\kappa=\frac{K_{ArOH}}{K_{ZH}}$ (we note that, in the bulk, $b^0=\frac{\kappa}{1+\kappa}$)

and therefore using the a_0, b_0 and z_0, zh_0 relationships already established:

$$z_0=\frac{2z^0b_0}{(1-\kappa)b_0+\kappa(1-\mathcal{I}\psi)}$$

Therefore:

$$b_0+\delta\frac{2z^0b_0}{(1-\kappa)b_0+\kappa(1-\mathcal{I}\psi)}=\frac{\kappa}{1+\kappa}+\delta_Z z^0-\mathcal{I}\psi$$

This equation can be simplified since in our case $\kappa=10^{-3}<<1$ (phosphate and phenol):

Finally leading to the dimensionless expression of the voltammetric responses:

$$\psi^{2/3}\exp\left(-\xi_{dim}\right)+\delta_Z\frac{2z^0\psi^{2/3}\exp\left(-\xi_{dim}\right)}{\psi^{2/3}\exp\left(-\xi_{dim}\right)+\kappa(1-\mathcal{I}\psi)}=\delta_Z z^0-\mathcal{I}\psi \qquad (3S)$$

providing (see section 3.6) the successful simulations shown in figures 5a and b.

Since $\kappa=K_{ArOH}/K_{ZH}$ is the ratio between to acid dissociation constants, it is not expected to vary significantly from H_2O to D_2O.

3.5. The PO_4H^{2-}-CPET pathway

We establish here the conclusion that, in the buffer concentration range relevant to the results displayed in figures 5a and b, the voltammetric response for the PO_4H^{2-}-CPET pathway is kinetically controlled by the CPET electron transfer owing to the involvement buffer concentration in the framework of a termolecular process (the electrode+ two molecules) in both directions.

With the same initial and boundary conditions as earlier and, noting that in the considered *pH* range ($pH << pK_{ArOH}$), the pertinent dimensionless partial derivatives equations are now:

$\frac{\partial a}{\partial\tau}=\frac{\partial^2 a}{\partial y^2}$, leading, after integration to: $a_0=1-\mathcal{I}\psi$.

$$\frac{\partial h}{\partial \tau}=\delta_H\frac{\partial^2 h}{\partial y^2}-\lambda_+ h\times z+\lambda_- zh,\ \frac{\partial z}{\partial \tau}=\delta_Z\frac{\partial^2 z}{\partial y^2}-\lambda_+ h\times z+\lambda_- h\times z,\ \frac{\partial zh}{\partial \tau}=\delta_Z\frac{\partial^2 zh}{\partial y^2}+\lambda_+ h\times z-\lambda_- h\times z$$

where λ_+ and λ_- are the dimensionless rate constants the protonation and deprotonation associated with the buffer couple.

Combination of these three equations and integration leads to:

$$z_0-\delta_H h_0=z^0-\delta_H h^0-\frac{\mathcal{I}\psi}{\sqrt{\delta_Z}},zh_0+\delta_H h_0=zh^0+\delta_H h^0-\frac{\mathcal{I}\psi}{\sqrt{\delta_Z}}\quad (z_0+zh_0=z^0+zh^0)$$

Since the protonation and deprotonation reactions are fast, equilibrium is maintained:

$$\frac{h_0\times z_0}{zh_0}=\kappa\ (=K_Z/C^0)$$

With the simplification that $pH=pK_{ZH}$ and therefore $z^0=zh^0$:

$$z_0-\frac{2\delta_H\kappa}{z_0}=z^0-\frac{2\delta_H\kappa}{z^0}-\frac{\mathcal{I}\psi}{\sqrt{\delta_Z}}$$

In the conditions of our study, $\kappa<<1$, and therefore:

$$z_0\simeq z^0-\frac{\mathcal{I}\psi}{\sqrt{\delta}},\ zh_0=z^0+\frac{\mathcal{I}\psi}{\sqrt{\delta}}$$

Dimerization of the phenoxyl radicals is involved in the same way as in the preceding section, leading similarly to $c_0=\left(3/2\lambda_{dim}\right)^{1/3}\psi^{2/3}$.

Applying now the dimensionless the Butler-Volmer law:

$$\psi=\Lambda\frac{C^0}{C_S}\exp\left(\frac{\xi}{2}\right)\left[a_0z_0-c_0zh_0\exp(-\xi)\right]\ \text{with:}\ \xi=\frac{F}{2RT}\left(E-E^{0,\mathrm{PO_4H^{2-}}}_{CPET}\right)\text{and}\ \Lambda=\frac{k^{CPET}_{S,\mathrm{PO_4H^{2-}}}}{\sqrt{D}\sqrt{\frac{Fv}{RT}}}$$

leads to:

$$\psi=\frac{\Lambda}{\left(\frac{2\lambda_{dim}}{3}\right)^{1/6}}\frac{Z^0}{C_S}\exp\left(\frac{\xi_{dim}}{2}\right)\left[(1-\mathcal{I}\psi)\left(1-\frac{\mathcal{I}\psi}{z^0\sqrt{\delta}}\right)-\psi^{2/3}\left(1+\frac{\mathcal{I}\psi}{z^0\sqrt{\delta}}\right)\exp(-\xi_{dim})\right]$$

with, as earlier: $\xi_{dim}=\xi+\frac{1}{3}\ln\left(\frac{2\lambda_{dim}}{3}\right)=\xi+\frac{1}{3}\ln\left(\frac{4k_{dim}C^0}{3}\frac{RT}{Fv}\right)$

There are two limiting case of interest:

Relatively large buffer concentrations, more precisely: $z^0>>\frac{\mathcal{I}\psi}{\sqrt{\delta_Z}}$, leading to:

$$\psi=p^{\textit{large buffer conc.}}_{,\mathrm{PO_4H^{2-}}-CPET}\exp\left(\frac{\xi_{dim}}{2}\right)\left[(1-\mathcal{I}\psi)-\psi^{2/3}\exp(-\xi_{dim})\right]$$

with an electron transfer/ dimerization competition parameter:

$$p^{\textit{large buffer conc.}}_{\mathrm{PO_4H^{2-}}-CPET}=\frac{\Lambda}{\left(\frac{2\lambda_{dim}}{3}\right)^{1/6}}\frac{Z^0}{C_S}=\frac{k^{CPET}_{S,\mathrm{PO_4H^{2-}}}Z^0}{D^{1/2}\left(\frac{Fv}{RT}\right)^{1/3}\left(\frac{4k_{dim}C^0}{3}\right)^{1/6}},$$

the involvement of the CPET pathway increasing, as expected, proportionally to the buffer concentration. In the conditions of the experiment in figure 5b ($Z^0=0.5$ mM), $k^{CPET}_{S,\mathrm{PO_4H^{2-}}}$ should be as large as 140 cm s^{-1} for the kinetic control to pass from electron transfer to dimerization. Since $k^{CPET}_{S,\mathrm{PO_4H^{2-}}}$ is obviously much smaller, we may conclude that the reaction is kinetically controlled by the CPET electron transfer step and should therefore exhibit a significant H/D isotope effect, if this pathway were actually followed.

In the converse situation of low buffer concentrations, more precisely: $z^0<<\frac{\mathcal{I}\psi}{\sqrt{\delta_Z}}$:

$$\psi'=p^{\textit{low buffer conc.}}_{\mathrm{PO_4H^{2-}}-CPET}\exp\left(\frac{\xi'_{dim}}{2}\right)\left[(1-\mathcal{I}\psi')-\psi'^{2/3}(1+\mathcal{I}\psi')\exp(-\xi'_{dim})\right]$$

with: $\psi'=\frac{\psi}{z^0\sqrt{\delta_Z}}$, $\xi'_{dim}=\xi_{dim}-\frac{2}{3}\ln\left(z^0\sqrt{\delta_Z}\right)$ and a competition parameter:

$$p^{\textit{low buffer conc.}}_{PO_4H^{2-}-CPET} = \frac{\Lambda Z^{0^{1/3}}}{\left(\frac{2\lambda_{dim}}{3}\right)^{1/6}\delta_Z{}^{1/3}}\frac{C^{0^{2/3}}}{C_S} = \frac{k_S^{CPET}\,\frac{Z^{0^{1/3}}C^{0^{2/3}}}{C_S}}{D^{1/6}D_Z{}^{1/3}\left(\frac{Fv}{RT}\right)^{1/3}\left(\frac{4k_{dim}C^0}{3}\right)^{1/6}}$$

In the conditions of the experiment in figure 5b ($Z^0 = 0.5$ mM), $k^{CPET}_{S,PO_4H^{2-}}$ should be as large as 240 cm s^{-1} for the kinetic control to pass from electron transfer to dimerization. Since $k^{CPET}_{S,PO_4H^{2-}}$ is obviously much smaller, we may conclude that the reaction is kinetically controlled by the CPET electron transfer step and should therefore exhibit a significant H/D isotope effect.

At 0.5 mM buffer, the situation is actually midway between the above two estimations leading to the same conclusion as to the prediction of a significant H/D isotope effect, if the PO_4H^{2-}-CPET pathway were actually followed.

3.6. Procedures for numerical simulations

3.6.1. Calculation of $\mathcal{I}\psi$

The integral domain is divided into small intervals within which the current is approximated by a linear function between the values at the ends of the interval. τ is divided into *p* divisions with width *h*:.

$$\mathcal{I}\psi = \frac{1}{\sqrt{\pi}}\int_0^{\tau}\frac{\psi(\eta)}{\sqrt{\tau-\eta}}d\eta = \frac{1}{\sqrt{\pi}h}\sum_{j=1}^{n}\int_{\tau_{j-1}}^{\tau_j}\frac{\psi_j\left(\eta-\tau_{j-1}\right)+\psi_j\left(\tau_j-\eta\right)}{\sqrt{\tau_n-\eta}}d\eta$$

thus:

$$\mathcal{I}\psi = \mathcal{I}_n = \mathcal{I}_{n-1} + \frac{1}{\sqrt{\pi}h}\int_{\tau_{p-1}}^{\tau_n}\frac{\psi_n\left(\eta-\tau_{p-1}\right)+\psi_n\left(\tau_n-\eta\right)}{\sqrt{\tau_n-\eta}}d\eta = \mathcal{I}_{n-1} + \frac{2}{3}\sqrt{\frac{h}{\pi}}\psi_{n-1} + \frac{4}{3}\sqrt{\frac{h}{\pi}}\psi_n$$

and

$$\mathcal{I}_{n-1} = \sqrt{\frac{h}{\pi}}\sum_{j=1}^{n}\frac{2}{3}\left(\psi_{j-1}-\psi_j\right)\left[\left(n-j+1\right)^{3/2}-\left(n-j\right)^{3/2}\right]+2\left[\psi_j\left(n-j+1\right)-\psi_{j-1}\left(n-j\right)\right]\left(\sqrt{n-j+1}-\sqrt{n-j}\right)$$

3.6.2. Numerical simulations for H_2O-CPET:

Starting with equation (2S):

$\psi = p\exp\left(\frac{\xi^*_{dim}}{2}\right)\left[1-\mathcal{I}\psi-\psi^{2/3}\mathcal{I}\psi\exp\left(-\xi^*_{dim}\right)\right]$ The general equation of the voltammetric response is :

$$\psi = p\exp\left(\frac{\xi'}{2}\right)\left\{1-\mathcal{I}_\psi-\psi^{2/3}\left(h^0\sqrt{\delta}+\mathcal{I}_\psi\right)\exp\left(-\xi'\right)\right\}$$

The current may be approximated by a linear function between the values at the ends of the interval, since the integral domain is divided into small intervals. τ is divided into *n* intervals of width *h*:

$$\frac{\psi_n}{p}\exp\left(-\frac{\xi^*_{dim}}{2}\right) = 1-\mathcal{I}_n\left[1+\psi_n^{2/3}\exp\left(-\xi^*_{dim}\right)\right]$$

with

$$\mathcal{I}_n = \mathcal{I}_{n-1} + \frac{2}{3}\sqrt{\frac{h}{\pi}}\psi_{n-1} + \frac{4}{3}\sqrt{\frac{h}{\pi}}\psi_n$$

Thus

$$\frac{\psi_n}{p}\exp\left(-\frac{\xi^*_{dim}}{2}\right) = 1-\left(\mathcal{I}_{n-1}+\frac{2}{3}\sqrt{\frac{h}{\pi}}\psi_{n-1}+\frac{4}{3}\sqrt{\frac{h}{\pi}}\psi_n\right)\left[1+\psi_n^{2/3}\exp\left(-\xi^*_{dim}\right)\right]$$

$$\psi_n^{5/3}\left[\frac{4}{3}\sqrt{\frac{h}{\pi}}\exp\left(-\xi^*_{dim}\right)\right]+\psi_n\left[\frac{\exp\left(-\frac{\xi^*_{dim}}{2}\right)}{p}+\frac{4}{3}\sqrt{\frac{h}{\pi}}\right]-\left[1-\mathcal{I}'_{n-1}\right]=0$$

with $\mathcal{I}'_{n-1} = \mathcal{I}_{n-1} + \frac{2}{3}\sqrt{\frac{h}{\pi}}\psi_{n-1}$

This non-linear algebraic equation has the following form.

$$\psi_p^{5/3} + \psi_p^{2/3}A + \psi_p B = C$$

where *A*, *B* and *C* depends on the previously computed values of the ψ function. These equations were solved by the "chord" iteration technique, noting that the solution sought is unique in the interval [0 - *C*/*B*], so that these two limits can be taken as starting values for the iteration.

3.6.3. Numerical simulations for OH^--PET:

The ψ value at a given ξ_{dim} is given by equation:

$$\frac{\psi^{2/3}\exp\left(-\xi_{dim}\right)}{1-\mathcal{I}\psi-\psi^{2/3}\exp\left(-\xi_{dim}\right)}=\frac{\kappa}{\delta}\left(\frac{\kappa oh^0}{1+\kappa oh^0}-\psi^{2/3}\exp\left(-\xi_{dim}\right)-\mathcal{I}\psi\right)+\kappa oh^0$$

or by the coupled equations:

$$b_0=\left(1-\mathcal{I}\psi\right)\frac{\frac{\kappa}{\delta_{OH}}\left(\frac{\kappa oh^0}{1+\kappa oh^0}-b_0-\mathcal{I}\psi\right)+\kappa oh^0}{1+\frac{\kappa}{\delta_{OH}}\left(\frac{\kappa oh^0}{1+\kappa oh^0}-b_0-\mathcal{I}\psi\right)+\kappa oh^0} \qquad (4S)$$

$$b^0-b_0=b^0-\psi^{2/3}\exp\left(-\xi_{dim}\right) \qquad (5S)$$

The numerical simulation is done by an iterative solving of the coupled equations: $\mathcal{I}\psi$ is first calculated taking $\psi_n=\psi_{n-1}$, leading to $\mathcal{I}\psi=\mathcal{I}_n=\mathcal{I}_{n-1}+2\sqrt{\frac{h}{\pi}}\psi_{n-1}$. b_0 is then calculated by means of equation (4S) and ψ_n by means of equation (5S). $\mathcal{I}\psi$ is recalculated next taking this new ψ_n value into account and the whole procedure is restarted until convergence for ψ_n is reached.

A similar procedure was followed to solve numerically equation (3S) in the PO_4H^{2-}-PET case.

References

1S. Krezel A, Bal W (2004) A formula for correlating *pKa* values determined in D_2O and H_2O. J. Inorg. Biochem. 98:161-166.
2S. Bhugun I, Savéant J-M (1995) Derivatization of surfaces and self-inhibition in irreversible electrochemical reactions: Cyclic voltammetry and preparative-scale electrolysis. J. Electroanal. Chem. 395:127-131.
3S. Savéant, J.-M. *Elements of Molecular and Biomolecular Electrochemistry,* Wiley-Interscience, New York, 2006, Chap. 1.
4S. Savéant, J.-M. *Elements of Molecular and Biomolecular Electrochemistry,* Wiley-Interscience, New York, 2006, Chap. 2.
5S. Rudolph M (2003) Digital simulations on unequally spaced grids.: Part 2. Using the box method by discretisation on a transformed equally spaced grid. J. Electroanal. Chem. 543:23-39.
6S. Savéant, J.-M. (2000) Dissociative electron transfer and the principle of microscopic reversibility. J. Electroanal. Chem. 485: 86-88.
7S. Savéant, J.-M. *Elements of Molecular and Biomolecular Electrochemistry,* Wiley-Interscience, New York, 2006, Chap. 3.